Taking advantage of electric field induced bacterial aggregation for the study of interactions between bacteria and macromolecules by capillary electrophoresis

Nicolas Sisavath, Patrice Got, Guillaume Charrière, Delphine Destoumieux-Garzón, Hervé Cottet

ANALYTICAL CHEMISTRY (2015) vol 87 pp 6761-6768

Taking Advantage of Electric Field Induced Bacterial Aggregation for the Study of Interactions between Bacteria and Macromolecules by Capillary Electrophoresis

Nicolas Sisavath,† Patrice Got,‡ Guillaume M. Charrière, § Delphine Destoumieux-Garzon,§ and HervéCottet*,†

† Institut des Biomolecules Max Mousseron (IBMM, UMR 5247 CNRS, Université de Montpellier, Ecole Nationale Superieure de Chimie de Montpellier), Place Eugene Bataillon, CC 1706, 34095 Montpellier, France
‡ Marine Biodiversity Exploitation & Conservation (MARBEC, UMR 9190), IRD, CNRS, IFREMER, Université de Montpellier, 34095 Montpellier, France
§ Interactions Hôtes-Pathogenes-Environnements (IHPE, UMR 5244), CNRS, Ifremer, Université de Perpignan Via Domitia, Université de Montpellier, Place Eugene Bataillon, CC 80, 34095 Montpellier, France

Abstract
The quantification of interaction stoichiometry and binding constant between bacteria (or other microorganism) and (macro)molecules remains a challenging issue for which only a few adapted methods are available. In this paper, a new methodology was developed for the determination of the interaction stoichiometry and binding constant between bacteria and (macro)- molecules. The originality of this work is to take advantage of the bacterial aggregation phenomenon to directly quantify the free ligand concentration in equilibrated bacteria-ligand mixtures using frontal analysis continuous capillary electrophoresis. The described methodology does not require any sample preparation such as filtration step or centrifugation. It was applied to the study of interactions between *Erwinia carotovora* and different generations of dendrigraft poly-L-lysines leading to quantitative information (i.e., stoichiometry and binding site constant). High stoichiometries in the order of 10^6 −10^7 were determined between nanometric dendrimer-like ligands and the rod-shaped micrometric bacteria. The effect of the dendrimer generation on the binding constant and the stoichiometry is discussed. Stoichiometries were compared with those obtained by replacing the bacteria by polystyrene microbeads to demonstrate the internalization of the ligands inside the bacteria and the increase of the specific surface via the formation of vesicles.

The study of noncovalent binding between (macro)- molecules and/or proteins is of primary interest in many fields, notably for the study and understanding of biochemical mechanisms,[1] and for the development of biological/pharmaceutical applications.[2,3] In microbiology, the study of interactions between microorganisms (bacteria, viruses, fungi, ...) and small molecules or macromolecules could be very useful to investigate antibacterial activity and/or ligand targeting ability. To meet this end, traditional techniques include microscopy methods,[4] surface plasmon resonance (SPR),[5] whole cell Systematic evolution of ligands by exponential enrichment (SELEX) coupled to flow cytometry,[6,7] and serological methods.[8,9] However, very few analytical techniques can bring quantitative information such as the stoichiometry and the constant of interaction between a microorganism and (macro)molecular ligands. Techniques of microscopy provide structural information on cell membrane integrity[10,11] but do not give access to interaction parameters. The whole cell SELEX process is useful to discriminate aptamers presenting high affinity for a bacterial strain but requires the coupling with flow cytometry to determine an association constant between both partners.[12,13] The stoichiometry of the

complex cannot be measured by this method. The main drawbacks of SPR and serological methods come from the necessity to immobilize one of the partners onto a surface.[14] This can generate a loss of the native bioactivity and a diminishing of the accessible active group leading to an underestimation of the stoichiometry. The proximity between species immobilized on the surface can also produce steric hindrance for the binding between partner. Moreover, nonspecific adsorption to the metal surface can lead to false signals.[15]

As capillary electrophoresis (CE) is a separation technique working in liquid phase, without stationary phase, it was also proposed as a promising technique to investigate interactions between bacteria (or microorganism) and (macro)molecules.

Since the pioneering work of Hjerten et al.′ [16] showing the electromigration of tobacco mosaic virus and *Lactobacillus casei* through a capillary, different CE methodologies and microbial assays were developed. For instance, CE has been used to determine viability of bacteria,[17] microbial contamination in biological samples,[18] or for quick sterility test.[19] As the mechanism of action of antimicrobial agents commonly begins by the membrane adhesion, many works investigated the use of CE to study the interaction between drugs and microbial receptors[20−23] or with liposomes simulating membranes[24−26] or directly with the whole living cells.[27−32] In this latter case, Armstrong et al. used affinity capillary electrophoresis (ACE) to study the interaction of *Bifidobacterium infantis* with Lucifer yellow and vancomycin.[27] Different concentrations of *B. infantis* were added in the running buffer, and the measurement of the ligand electrophoretic mobility led to the determination of an apparent binding constant of 1.1 × 1013 M−1 . Ding et al. have also used ACE to determine the equilibrium constant between living *Staphylococcus aureus* and antimicrobial peptides.[29,30] The authors measured similar values as that found by Armstrong.[27] Nevertheless, it is worth noting that ACE does not allow determining quantitative information on the complex stoichiometry. Kenndler and co-workers have also worked intensively on the study of interactions between viruses and ligands by CE.[14,33,34] They developed a model of data treatment based on the thermodynamic of complex formation in order to determine the stoichiometry and the dissociation constant.[34]

One major limitation in the use of CE for the study and characterization of bacteria, and more generally microorganisms, is the occurrence of aggregation phenomenon. Bacteria have a natural tendency to aggregate under clusters of random sizes[35] presenting different electrophoretic mobilities. Zheng et al.[36] noticed that the aggregation was promoted by the occurrence of multiple collisions between bacteria during the electrophoretic migration. The presence of such aggregates leads to typical haired-shaped profiles (spikes) as described by Petr et al.[37] This uncontrollable aggregation observed in capillary zone electrophoresis (CZE) was responsible for unreproducible analysis of bacteria.[38] Subsequently, research efforts have been carried out to try to improve the reproducibility of microbial analysis. Among them, we can cite the use of poly(ethylene oxide) (PEO)[39−42] or cationic surfactant (CTAB)[19] and methods based on the focusing of the injected analyte, such as isotachophoresis.[38,43−47] Capillary isoelectric focusing (cIEF) was also found very effective and repeatable to separate different bacterial strains according to their surface charge or isoelectric point.[48−51]

Recently, a new antibacterial assay based on anionic isotachophoresis (ITP) and multiple UV detection points using CE equipment was developed.[32] The antibacterial activity of cationic molecules on bacteria (Gram-positive and Gramnegative) was studied by detecting the bacteria before, during, and after their meeting with the antibacterial compound. This approach was useful to study the fast bacteriolytic activity of cationic compounds or to demonstrate the adsorption of cationic molecules onto bacteria.

Using a different approach, Schwartz et al.[52] used ITP for focusing cationic antimicrobial peptides as fluorescent labels for the detection and the quantification of bacterial species by a microfluidic assay.

Despite these recent developments, there is still a need for analytical methods allowing the quantitative determination of stoichiometry and affinity constant for microorganism-ligand interactions. In this work, we propose to take advantage of the bacterial aggregation in frontal analysis continuous capillary electrophoresis (FACCE)[53] for the quantitative study of bacteria-ligand interactions. Stoichiometry and binding constant of the interactions between *E. carotovora* and different generations of dendrigraft poly-L-lysines (DGL) are determined using this new approach. DGL were selected as ligands since they are known to have high affinity toward bacteria. It was also demontrated that DGL did not lysed *E. carotovora* contrary to *M. luteus*. [32] The influence of dendrimer generation on the bacteria-ligand interaction is discussed.

THEORY

In the present work, the bacteria is considered as the substrate S, and the DGL as the ligand L. n stands for the maximum number of binding sites on the substrate which can be very high in the case of bacteria-macromolecules interactions due to the aspect ratio between the two partners. The equilibrium between L and S can be described as

$$S + nL \leftrightarrow SL_n \tag{1}$$

where β_n is the equilibrium constant and is given by

$$\beta_n = \frac{[SL_n]}{[S][L]^n} \tag{2}$$

where $[S]$ and $[L]$ are the free substrate and ligand concentrations, respectively, and $[SL_n]$ is the concentration of SL_n complex. The average number of bound ligands per substrate $\bar{n}$ can be calculated from eq 3

$$\bar{n} = \frac{[L]_{tot} - [L]}{[S]_{tot}} \tag{3}$$

where $[L]_{tot}$ and $[S]_{tot}$ are the initial concentrations in ligand and substrate introduced in the mixture. $[L]$ is the free ligand concentration which can be experimentally determined by FACCE. The adsorption isotherm is defined as the plot of $\bar{n}$ versus $[L]$ and should follow eq 4 in the case of n independent sites of equal energy:

$$\bar{n} = n\frac{k[L]}{1 + k[L]} \tag{4}$$

k represents the binding site constant, with $\beta_n = k^n$. The binding site constant k should not be confused with the successive equilibrium constant K_i defined by eq 5:

$$SL_{i-1} + L \leftrightarrow SL_i \tag{5}$$

The relationship between k and K_i is given by the following equation, based on statistical considerations:

$$K_i = \frac{n - i + 1}{i}k \tag{6}$$

The determination of the interaction parameters (k, n) is generally obtained by a curve fitting of the isotherm of adsorption $\bar{n} = f([L])$ using eq 4. The isotherm of adsorption is experimentally plotted by determining the free ligand concentration $[L]$ by FACCE for different mixtures containing different initial substrate–ligand concentrations.

EXPERIMENTAL SECTION

Chemical and Polymers.

Acetic acid, glacial, Tris 99.9% $(HOCH_2)_3CNH_2$, PDADMAC (poly diallyl dimethyl amonium chloride) (M_w = 400−500 kDa), sodium chloride, and Luria− Bertani (LB) agar plates were purchased from Sigma-Aldrich (Steinheim, Germany). The bacteria *Erwinia carotovora* were kindly provided by the Lagoon Ecosystems laboratory, UniversitéMontpellier 2 (Montpellier, France). Syringe filters in cellulose acetate membrane with 0.2 µm pore size were purchased from VWR. Deionized water was further purified using a Milli-Q system (Millipore, Molsheim, France). DGL (G_2-G_5) (lot nos. DC 1210-02B; DC1201-03; DC 1201-04 and DC 1201-05, respectively) were supplied by COLCOM (Montpellier, France). DGL of generation 2 to 5 are ramified synthetic polypeptides only constituted of lysine and, thus, highly cationic macromolecules.[54] Polystyrene microbeads were purchased from Polysciences Europe GmbH (Eppelheim, Germany) (lot no. 597936, 952.8 ± 12 nm diameter). Other chemicals were of reagent grade and used without further purification

Bacterial Growth Conditions and Sample Preparation.

The bacteria were maintained under standardized growth conditions: one colony of *Erwinia carotovara* was transferred from Luria−Bertani (LB) agar plates into Erlenmeyer flasks containing 8 mL of LB liquid medium. The flasks were incubated for 13 h at 37 °C with constant agitation (120 rpm) on a rotary platform shaker for good aeration. Fresh liquid cultures were prepared daily. To separate the bacteria from the medium, the suspension in the flasks was centrifuged (model: SIGMA 3K12, Larborzentrifugen, Osterode, Germany) at 150g for 15 min to get the bacteria in pellet form. The supernatant was removed carefully, and the pellet was resuspended by vortexing for 30 s in 8 mL of CE buffer filtered on a 0.45 µm size pore membrane. Then, the bacteria suspension was centrifuged for 15 min. This washing process was repeated twice. Eight milliliters of filtered CE buffer were added to the washed bacteria cells and vortexed until the bacterial pellets were completely resuspended.

Preparation of DGL-E. carotovora or DGL-Microbeads Mixtures.

Bacterial suspensions were prepared as above and resuspended in Tris buffer (8 mM Tris, 6.5 mM AcOH, 6.5 mM ionic strength, pH 7.4) at room temperature. Stock solutions of DGL (G_2: 0.4 mg/mL, i.e. 34.4 µM, G_3: 0.4 mg/ mL, i.e. 13.4 µM, G_4: 0.4 mg/mL, i.e. 4.53 µM and G_5: 0.4 mg/ mL, i.e. 1.72 µM) were prepared at room temperature in Tris buffer. DGL-*E. carotovora* mixtures for direct FACCE analysis (without filtration) were prepared by mixing the same volume (0.1 mL) of bacteria suspensions at ∼10^8 cells/mL and stock DGL solutions at different concentrations. The final concentrations after the 50/50 v/v mixture are as follows: DGL (G_2- G_5) at 0.2, 0.15, 0.1, 0.075, 0.05 0.0375, 0.025, and 0.0125 mg/ mL and bacteria (1.59 × 10^8 cells/mL, i.e. 2.6 × 10−13 M). G2- E. carotovora mixtures for analysis by the method with filtration were prepared following the same protocol with final concentrations in bacteria at (1.89 × 10^8 cells/mL, i.e. 3.14 × 10^{-13} M).

As for the experiments at physiological conditions, the bacteria and DGL solutions were prepared in Tris buffer. The protocol of preparation of the mixtures was the same as previously described with a final bacteria concentration of 1.14 × 10^8 cells/mL (i.e., 3.79 × 10^{-13} M).

DGL-PS microbeads mixtures were prepared by mixing the same volume (0.4 mL) of PS microbeads solution at constant concentration and stock DGL solutions at different concentrations. PS microbeads solutions and DGL solutions were prepared in Tris buffer. The final concentrations in the mixtures are PS microbeads at 3.93×10^{-12} M with DGL at 0.2, 0.15, 0.1, 0.075, 0.05, 0.0375, and 0.025 mg/mL. The DGL-PS microbeads mixtures were filtered prior analyses on cellulose acetate membrane syringe filters with 0.2 μm pore size.

Frontal Analysis Continuous Capillary Electrophoresis.

FACCE experiments were carried out using a 3D-CE Agilent system (Waldbronn, Germany) equipped with a diode array detector. Bare fused silica capillaries (50 μm i.d. × 8.5 cm (to the detector) × 33.5 cm) were purchased from Composite Metal Services (Worcester, U.K.). The background electrolytes (BGE) for FACCE analysis were our standard 6.5 mM ionic strength Tris buffer (8 mM Tris, 6.5 mM AcOH, pH 7.4) and a 154 mM ionic strength Tris buffer in which 147.5 mM NaCl were added. New fused silica capillaries were first flushed with NaOH (1M) for 30 min, water for 10 min, 0.2% (w/w) PDADMAC solution in water for 30 min, BGE for 10 min. A +30 kV (respectively +2 kV) voltage was applied for the 6.5 mM (respectively 154 mM) ionic strength Tris buffer for 10 min. The conditioning between two successive runs was done according to the following protocol: water for 2 min, 0.2% (w/ w) PDADMAC in water for 2 min, and then BGE for 2 min.

The temperature of the capillary cartridge was set at 25 °C. To limit the effective length to 8.5 cm, the sample was introduced from the capillary end which is the closest to the detection point (outlet end). FACCE of DGL (G_2 to G_5) was realized by applying a normal polarity voltage (from the injection end) of +2.5 kV and a +10 mbar copressure (from injection end) for analyses of DGL-*E. carotovora* mixtures in 8 mM Tris buffer. Analyses of DGL-*E. carotovora* mixtures in 8 mM Tris buffer containing 147.5 mM NaCl were performed by applying a normal polarity voltage of +1 kV and a +5 mbar copressure.

Analyses of DGL-PS Microbeads mixtures were performed by applying a normal polarity voltage of +2.5 kV and a +20 mbar copressure from injection end. Each analysis was performed in triplicate.

RESULTS AND DISCUSSION

Taking Advantage of Aggregation of Bacteria for the Quantification of Free Ligand by Frontal Analysis Continuous Capillary Electrophoresis.

As stated in the theoretical section, plotting the isotherm of adsorption requires the determination of the free ligand [L] at equilibrium in various substrate−ligand mixtures. This was done by frontal analysis continuous capillary electrophoresis (FACCE) which consists in injecting continuously the equilibrated sample mixture from one end of the capillary by applying a constant electric field. The equilibrated mixture is prepared in the same electrolyte as the background electrolyte (8 mM Tris + 6.5 mM acetic acid at pH 7.4). A polycationic capillary coating was used to avoid any adsorption of the ligand or the bacteria-DGL complex onto the capillary surface. Indeed, the positive charge of the *E. carotovora*-DGL complex has been previously demonstrated by capillary zone electrophoresis.[32] A copressure was applied simultaneously with the positive voltage polarity to partially compensate the anodic electroosmotic flow (EOF) which is directed against the ligand migration.[55]

Examples of electropherograms obtained by FACCE are given in Figure 1B. The upper trace corresponds to a DGL solution (0.1 g/L G_2 without bacteria), and the lower trace was obtained for a DGL-bacteria mixture (0.1 g/L G_2 + bacteria at 1.59×10^8 cells/mL). In the absence of bacteria, DGL are detected as a front due to the continuous injection of the sample. The height of the plateau is proportional to the DGL concentration. For the DGL-bacteria mixture, we observe a DGL plateau on which multiple spikes appear. Each one of these spikes (see e.g. at $t = t_2$) corresponds to bacteria-DGL aggregates. Between

two spikes (see e.g. at $t = t_1$), the background absorbance corresponds to the free DGL concentration in the equilibrated mixture. It is worth noting that the aggregates should move sufficiently slowly in front of the detector to visualize the baseline return to the background absorbance between two spikes. To meet this end, the pressure has to be adjusted (see Figure SI2). The decrease in the front height in the presence of bacteria reflects a lower concentration in free DGL, which can be explained by their binding to bacteria. It is worth noting that a simple hydrodynamic mobilization of the DGL-bacteria mixture, without applied voltage, does not generate aggregates and spikes such as those observed in Figure 1 (see section 3 in the SI for more details).

Figure 1A gives a schematic representation of the detection at two different times (t_1 and t_2). It should be noted that, in the present case, the bacterial aggregation is beneficial for the detection of the free DGL concentration. If such aggregation would not take place, we could not differentiate free DGL from bacteria-DGL complexes, especially because bacteria-DGL complexes have multiple different mobilities according to their size and shape. As long as the difference in migration time between aggregates is sufficient to get a baseline return, the background absorbance (e.g., at $t = t_1$) is indicative of the free DGL concentration in solution. For a completely different application, it is worth noting that Viovy's group recently proposed to take advantage of DNA aggregation caused by electrohydrodynamic instabilities for the ultrasensitive detection of DNA in a very compact and low cost microchip.[56]

Isotherm of Adsorption of G_2 onto *E. carotovora*.

Figure 2A displays the FACCE traces obtained at different DGL (G_2) concentrations keeping constant the *E. carotovora* concentration at 1.59×10^8 cells/mL (i.e., 2.64×10^{-13} M).

The corresponding traces for the DGL alone at the same initial concentration are also displayed. The difference in DGL background absorbance in the presence/in the absence of bacteria is directly proportional to the concentration of bound DGL in the mixture. From the height of the plateaus obtained for the bacteria-DGL mixtures (Figure 2A), it is possible to quantify the free DGL concentrations at equilibrium and thus to plot the isotherm of adsorption (see black circles in Figure 2B). To ensure that bacterial counts were not affected by DGL, bacterial suspensions were counted by flow cytometry over the whole range of DGL concentrations used. A variation of 7− 24% of the bacterial population was observed after addition of DGL, which still corresponds to reasonable fluctuations for biological samples. These fluctuations have been taken into account for the error bars on $\bar{n}$ (see section 6 in the SI for more details). To confirm that the FACCE method leads to correct stoichiometry and binding constant; the same isotherm was determined by quantification of the free DGL after physical separation by filtration (see red squares in Figure 2B). By this way, the bacteria (and the attached DGL on it) are physically trapped onto the filter, and the free DGL was directly quantified by CE. Similar results were obtained with both methods (see Figure 2B for numerical values); with the advantage for the direct method that a filtration step was not required. The method with filtration requires also a higher sample volume (800 µL) due to the dead volume in the filter. Stoichiometry of about $1.0-1.1 \times 10^7$ G_2 per bacteria with an apparent binding site constant of $\sim 2-3 \times 10^6$ M^{-1} was obtained by curve fitting using eq 4.

Comparison between Different DGL Generations

The direct FACCE method (without filtration) was used to study the influence of DGL generation on the bacteria-DGL interaction. As for any dendritic macromolecule, the molar mass (or degree of polymerization) of the DGL increases exponentially with dendrimer generation number, while the hydrodynamic radius increases almost linearly from 1.0 (G_1) to 6.4 nm (G_5) (see Table 1 for numerical values). A previous work[57] which focused on DGL-human serum albumin (HSA) interactions showed

that higher DGL generations lead to stronger binding constants with HSA and lower stoichiometries (from 8:1 for G_1-HSA down to 1:1 for G_5).

The values of the stoichiometry and binding constant are gathered in Table 1 (isotherms of adsorption are provided in Figure SI4). As expected, the stoichiometry of the interaction (n) decreases with the generation number from n = 1.0 × 10^7 for G_2 down to n = 2.6 × 10^5 for G_5, in good correlation with an increase of the ligand size. However, it can be noticed that the number of lysine residues bound per cell remains constan from G_2 to G_4 (4.9 × 10^8 to 4.0 × 10^8). This comes from the fact that the increase of the polymerization degree with generation number compensates the decrease of the stoichiometry. On the contrary, the binding site constant k increases with the generation number from k ∼ 3.2(±0.9) × 10^6 M^{-1} for G_2 up to k ∼ 47(±7.0) × 10^6 M−1 for G_5. These results are comparable with those obtained for the interaction between antimicrobial compounds and D-Ala-D-Ala terminal groups present on the bacterial membrane. Binding constants for the interaction between vancomycin and N-Ac-Lys-D-Ala-DAla peptide have been found in a range of 9.1 × 10^5 M^{-1} [58] to 2.7 × 10^6 M^{-1} [59] (in 150 mM ionic strength phosphate buffer, pH 7.4). In the very few studies dealing with the interaction between (macro)molecules and whole living cells, apparent binding constants were in a range of 7.4 × 10^{11} M^{-1} [30] (antimicrobial peptide JCpep8 to *Staphylococcus aureus*) to 1.1 × 10^{13} M^{-1} (vancomycin to *Bifidobacterium infantis*).[27] These equilibrium constant values determined by ACE are much higher than those found in this work, but this is due to the fact that ACE does not give directly access to the binding site constant k but to an apparent constant that is more related to the first equilibrium constant K1 = n × k (see eq 6). Knowing the very high number of sites, this explains the differences in the binding site constant k ∼ 10^6 −10^7 M^{-1} and the apparent constant obtained by ACE K ∼ 10^{11}–10^{13} M^{-1} .

To get more insight on the experimental stoichiometries obtained for the DGL-*E. carotovora* interaction, the n values were compared with maximum theoretical values (nth) considering a coverage of the bacterial surface with an hexagonal close-packed monolayer.[60] n_{th} was calculated using eqs 7 and 8

$$\Gamma_{th} = \frac{0.87}{\pi R_h^2 N_A} \quad (7)$$

$$n_{th} = \Gamma_{th} \times S_{subs} \times N_A = \frac{0.87}{\pi R_h^2} \times S_{subs} \quad (8)$$

where R_h is the hydrodynamic radius of the DGL ligand, and NA is the Avogadro number. Γ_{th} (in mol/m^2) is the theoretical maximum density of ligand onto a surface considering a hexagonal close-packed monolayer. S_{subs} is the substrate (bacteria) surface evaluated to 7.85 × 10^{-12} m^2 (cylinder of 2 µm long and 500 nm radius). From Table 1, it appears that the experimental stoichiometries are about 10 to 20 times higher than the theoretical nth value. Different reasons may explain a higher experimental stoichiometry: (i) the internalization of the ligand into the bacteria; (ii) the formation of ligand multilayers onto the bacteria membrane, and (iii) the roughness of the bacteria surface at the scale of the ligand (a few nm) or the formation of vesicles at the surface of the bacteria that may drastically increase S_{subs}.

Comparison with Polystyrene Microbeads.

To evaluate the importance of the phenomena (i) and (iii) that could be specific to the bacteria, interactions of DGL with negatively charged polystyrene microbeads (∼1 µm diameter) were

investigated. The beads serve as a control on which DGL can be adsorbed but not internalized. The filtration method was used for determining the free DGL concentration in the mixtures, because the polystyrene microbeads do not aggregate under the influence of the electric field. Parameters of the DGLmicrobead interactions obtained by curve fitting of the isotherms of adsorption are gathered in Table 1 (isotherms are provided in Figure SI5). It appears that n/nth which varies between 2 and 5 (from G_5 to G_2) is still higher than 1 but in a much lesser extent compared to bacteria. This difference highlights the significant amount of DGL that can be adsorbed onto the bacteria due to the increase in specific surface area (roughness, vesicle formation) or internalized in the bacteria.

Actually, the ability of DGL, or derivatives, to cross lipidic membranes has already been reported for their DNA transfection ability.[61−63] The remaining excess of ligands compared to a purely geometrical coverage, which cannot be explained by internalization in the case of the microbeads, is most likely due to the roughness of the microbead surface at a DGL scale. Indeed, this excess decreases with increasing the generation number (and thus, with DGL size). Aggregation of DGL is very unlikely for G_2 and very limited for G_3. 54 Moreover, if aggregation was supposed to occur, this effect should increase with the generation number,[54] in contradiction with the decrease of the n/n_{th} ratio.

Electron Microscopy Experiments.
Supporting the hypothesis of vesicles formation at the surface of the bacteria, transmission electronic microscopy experiments were performed. Figure 3 displays the bacteria without (Figure 3a) and with DGL (Figure 3b) in Tris buffer and shows that bacteria have still their outer membranes despite the alterations caused by the DGL. Figure 3b confirms a massive release of outer membrane vesicles (OMVs) detaching from *E. carotovora* upon treatment with DGL. Their diameter is in the range of 80 to 100 nm. This phenomenon is known to be triggered by antimicrobial peptides in a defense mechanism of bacteria against the harmful properties of membrane active agents.[64,65]

Confocal Microscopy Experiments.
Figure 4 shows bacterial suspension in the presence of G_2 labeled covalently with carboxyfluorescein. After 1 h of incubation in the Tris buffer, the fluorescently labeled G_2 clearly appears inside the cytoplasmic space of bacteria.

In conclusion, DGL-bacteria stoichiometry is much higher than the theoretical expectations based on purely geometrical considerations. This can be explained by internalization of DGL into the bacteria and by the increase of specific bacteria surface due to the roughness of the surface and the formation of vesicles.

Determination of Interaction Parameters in Physiological Conditions.
Finally, the possibility to apply the direct frontal analysis CE method in physiological conditions has been investigated because most of the biologically relevant applications are performed at 154 mM ionic strength, pH 7.4. Experimental conditions were adapted for that purpose: the pressure was adjusted to 5 mbar in order to obtain the return to the background absorbance between the bacterial spikes, and the applied voltage was decreased to +1 kV to minimize Joule heating. The isotherm of adsorption obtained at 154 mM ionic strength in the case of the interaction between G_2 and *E. caratovora* (isotherm provided in Figure SI6) did not show significant differences for the stoichiometry compared with the study at low ionic strength. However, as expected in the case of electrostatic interactions, the binding site constant was decreased with increasing ionic strength. The binding site constant k was ∼3 times lower at physiological pH.

CONCLUSION

In this work, we demonstrated that taking advantage of the electric field-induced bacterial aggregation allows determining the stoichiometry and the binding site constant between polycation ligands and bacteria, by direct analysis of equilibrated mixtures using frontal analysis continuous capillary electrophoresis. This methodology does not require any filtration step nor sample treatment. The model of independent sites of equal energy was used to determine DGL-bacteria binding site constant k in the order of $\sim 10^6 - 10^7$ M^{-1} . Ligandsubstrate stoichiometries decrease with DGL generation number and are in the range of 0.26×10^6 to 10.2×10^6 . A comparative study with polystyrene microbeads showed that a large part of DGL was internalized into the bacteria and adsorbed in excess onto the bacteria due to an increase in the specific surface, via e.g. the formation of vesicles as observed by microscopy. Finally, the possibility to apply this method in physiological conditions has been demonstrated which opens up new opportunities for the quantitative analysis of microorganism-ligand interactions of biological relevance

ACKNOWLEDGMENTS

H.C. gratefully acknowledges the support from the Institut Universitaire de France and from the Region LanguedocRoussillon for the fellowship “Chercheurs d’Avenir”. We gratefully acknowledge Chatal Cazevieille (Centre de ressources en imagerie cellulaire, Montpellier) for precious help in the experiments of electron microscopy. We thank the Montpellier RIO Imaging platform for access to the confocal microscopy

REFERENCES

(1) Barabasi, A. L.; Oltvai, Z. N.́ Nat. Rev. Genet. 2004, 5 (2), 101− 113.
(2) Wishart, D. S.; Knox, C.; Guo, A. C.; Cheng, D.; Shrivastava, S.; Tzur, D.; Gautam, B.; Hassanali, M. Nucleic Acids Res. 2008, 36 (Database issue), 901−906.
(3) Alexis, F.; Pridgen, E.; Molnar, L. K.; Farokhzad, O. C. Mol. Pharmaceutics 2008, 5
(4), 505−515. (4) Martin, N. L.; Beveridge, T. J. Antimicrob. Agents Chemother. 1986, 29 (6), 1079−1087.
(5) Pourshafie, M. R.; Marklund, B.-I.; Ohlson, S. J. Microbiol. Methods 2004, 58 (3), 313−320.
(6) Hamula, C. L. A.; Zhang, H.; Guan, L. L.; Li, X. F.; Le, X. C. Anal. Chem. 2008, 80 (20), 7812−7819.
(7) Duan, N.; Wu, S.; Chen, X.; Huang, Y.; Wang, Z. J. Agric. Food Chem. 2012, 60, 4034−4038.
(8) Chen, C.; Ding, H.; Chang, T. J. Food Prot. 2001, 64 (3), 348− 354.
(9) Kumar, S.; Balakrishna, K.; Batra, H. V. Biomed. Environ. Sci. 2008, 21 (2), 137−143.
(10) Andersson, E.; Rydengard, V.; Sonesson, A.; Mo¨ rgelin, M.; Bjö rck, L.; Schmidtchen, A. Eur. J. Biochem. 2004, 271 (6), 1219− 1226.
(11) Joshi, S.; Dewangan, R. P.; Yadav, S.; Rawat, D. S.; Pasha, S. Org. Biomol. Chem. 2012, 10 (41), 8326−8335.
(12) Hamula, C. L. A.; Le, X. C.; Li, X. Anal. Chem. 2011, 83, 3640− 3647.
(13) Dwivedi, H. P.; Smiley, R. D.; Jaykus, L. A. Appl. Microbiol. Biotechnol. 2010, 87 (6), 2323−2334.
(14) Okun, V. M.; Moser, R.; Ronacher, B.; Kenndler, E.; Blaas, D. J. Biol. Chem. 2001, 276 (2), 1057−1062.
(15) Campbell, C. T.; Kim, G. Biomaterials 2007, 28 (15), 2380− 2392.
(16) Hjerten, S.; Elenbring, K.; Kilá r, F.; Liao, J. L.; Chen, A. J. C.;́ Siebert, C. J.; Zhu, M. D. J. Chromatogr. A 1987, 403, 47−61.
(17) Armstrong, D. W.; He, L. Anal. Chem. 2001, 73 (19), 4551− 4557.
(18) Tong, M.-Y.; Jiang, C.; Armstrong, D. W. J. Pharm. Biomed. Anal. 2010, 53 (1), 75−80.
(19) Rodriguez, M. A.; Lantz, A. W.; Armstrong, D. W. Anal. Chem. 2006, 78 (14), 4759−4767.
(20) Mito, E.; Gomez, F. A. Chromatographia 1999, 50 (11), 689− 694.
(21) Heintz, J.; Hernandez, M.; Gomez, F. A. J. Chromatogr. A 1999, 840 (2), 261−268.

(22) Liu, X.; Gomez, F. A. Anal. Bioanal. Chem. 2009, 393 (2), 615− 621.
(23) Azad, M.; Brown, A.; Silva, I.; Gomez, F. A. Anal. Bioanal. Chem. 2004, 379 (1), 149−155.
(24) Helle, A.; Makitalo, J.; Huhtanen, J.; Holopainen, J. M.;¨ Wiedmer, S. K. Biochim. Biophys. Acta 2008, 1778 (11), 2640−2647.
(25) Carrozzino, J. M.; Khaledi, M. G. Pharm. Res. 2004, 21 (12), 2327−2335.
(26) Lucio, M.; Lima, J. L. F. C.; Reis, S. Curr. Med. Chem. 2010, 17 (17), 1795−1809.
(27) Berthod, A.; Armstrong, D. W. Electrophoresis 2002, 23, 847− 857.
(28) Meng, C.; Zhao, X.; Qu, F.; Mei, F.; Gu, L. J. Chromatogr. A 2014, 1358, 269−276.
(29) Xiao, J.; Zhang, H.; Niu, L.; Ding, S. Anal. Methods 2011, 3 (11), 2579.
(30) Xiao, J.; Zhang, H.; Ding, S. J. Agric. Food Chem. 2012, 60 (18), 4535−4541.
(31) Kłodzińska, E.; Jaworski, M.; Kupczyk, W.; Jackowski, M.; Buszewski, B. Electrophoresis 2012, 33 (19−20), 3095−3100.
(32) Oukacine, F.; Romestand, B.; Goodall, D. M.; Massiera, G.; Garrelly, L.; Cottet, H. Anal. Chem. 2012, 84 (7), 3302−3310.
(33) Okun, V. M.; Ronacher, B.; Blaas, D.; Kenndler, E. Anal. Chem. 2000, 72 (19), 4634−4639.
(34) Okun, V. M.; Moser, R.; Blaas, D.; Kenndler, E. Anal. Chem. 2001, 73 (16), 3900−3906.
(35) Szumski, M.; Kłodzińska, E.; Buszewski, B. J. Chromatogr. A 2005, 1084 (1−2), 186−193.
(36) Zheng, J.; Yeung, E. S. Anal. Chem. 2003, 75 (4), 818−824.
(37) Petr, J.; Ryparova, O.; Znaleziona, J.; Maier, V.; Sevcík, J.́ Electrophoresis 2009, 30 (22), 3863−3869.
(38) Oukacine, F.; Garrelly, L.; Romestand, B.; Goodall, D. M.; Zou, T.; Cottet, H. Anal. Chem. 2011, 83 (5), 1571−1578.
(39) Armstrong, D. W.; Schulte, G.; Schneiderheinze, J. M.; Westenberg, D. J. Anal. Chem. 1999, 71 (24), 5465−5469.
(40) Buszewski, B.; Kłodzińska, E. Electrophoresis 2008, 29 (20), 4177−4184.
(41) Jackowski, M.; Szeliga, J.; Kłodzińska, E.; Buszewski, B. Anal. Bioanal. Chem. 2008, 391 (6), 2153−2160.
(42) García-Cañ as, V.; Cifuentes, A. Electrophoresis 2007, 28 (22), 4013−4030.
(43) Yu, L.; Li, S. F. Y. J. Chromatogr. A 2007, 1161 (1−2), 308−313.
(44) Petr, J.; Jiang, C.; Sevcik, J.; Tesarova, E.; Armstrong, D. W. Electrophoresis 2009, 30 (22), 3870−3876.
(45) Oukacine, F.; Quirino, J. P.; Destoumieux-Garzon, D.; Cottet,́ H. J. Chromatogr. A 2012, 1268, 180−184.
(46) Phung, S. C.; Nai, Y. H.; Powell, S. M.; Macka, M.; Breadmore, M. C. Electrophoresis 2013, 34 (11), 1657−1662.
(47) Dziubakiewicz, E.; Buszewski, B. Electrophoresis 2014, 35 (8), 1160−1164.
(48) Horka, M.; Ruˇ zicka, F.; Horky, J.; Holaˇ , V.; Slais, K.́ J. Chromatogr. B: Anal. Technol. Biomed. Life Sci. 2006, 841 (1−2), 152− 159.
(49) Ruzicka, F.; Horka, M.; Hola, V.; Votava, M. J. Microbiol. Methods 2007, 68 (3), 530−535.
(50) Horka, M.; Horkýˇ , J.; Matouskovaˇ , H.; Slais, K.́ J. Chromatogr. A 2009, 1216 (6), 1019−1024.
(51) Vykydalova, M.; Horkaˇ , M.; Ruˇ zič ka, F.; Dusˇ a, F.; Moravcovaˇ ´, D.; Kahle, V.; Slais, K. Anal. Chim. Acta 2014, 812, 243−249.
(52) Schwartz, O.; Bercovici, M. Anal. Chem. 2014, 86, 10106− 10113.
(53) Gao, J. Y.; Dubin, P. L.; Muhoberac, B. B. Anal. Chem. 1997, 69 (15), 2945−2951.
(54) Martin, M.; Papillaud, A.; Souaıd, E.; Collet, H.; Commeyras, A. Biomacromolecules 2007, 8, 3235−3243.
(55) Sisavath, N.; Leclercq, L.; Le Saux, T.; Oukacine, F.; Cottet, H. J. Chromatogr. A 2013, 1289, 127−132.

(56) Diakite, M. L. Y.; Champ, J.; Descroix, S.; Malaquin, L.; Amblard, F.; Viovy, J. L. Lab Chip 2012, 12 (22), 4738−4747.
(57) Sisavath, N.; Le Saux, T.; Leclercq, L.; Cottet, H. Langmuir 2014, 30 (15), 4450−4457.
(58) Rao, J.; Yan, L.; Xu, B.; Whitesides, G. M. J. Am. Chem. Soc. 1999, No. 16, 2629−2630. (59) Lahiri, J.; Isaacs, L.; Tien, J.; Whitesides, G. M. Anal. Chem. 1999, 71 (4), 777−790.
(60) Herzog, G.; Flynn, S.; Johnson, C.; Arrigan, D. W. M. Anal. Chem. 2012, 84, 5693−5699.
(61) Hofman, J.; Buncek, M.; Haluza, R.; Streinz, L.; Ledvina, M.; Cigler, P. Macromol. Biosci. 2013, 13 (2), 167−176.
(62) Huang, R.; Liu, S.; Shao, K.; Han, L.; Ke, W.; Liu, Y.; Li, J.; Huang, S.; Jiang, C. Nanotechnology 2010, 21 (26), 265101.
(63) Tsogas, I.; Theodossiou, T.; Sideratou, Z.; Paleos, C. M.; Collet, H.; Rossi, J. C.; Romestand, B.; Commeyras, A. Biomacromolecules 2007, 8 (10), 3263−3270.
(64) Manning, A. J.; Kuehn, M. J. BMC Microbiol. 2011, 11 (1), 258.
(65) Destoumieux-Garzon, D.; Duperthuy, M.; Vanhove, A. S.; Schmitt, P.; Wai, S. N. Antibiotics 2014, 3, 540−563.

FIGURES

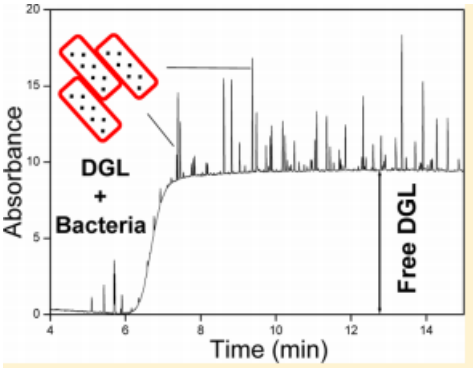

Abstract figure

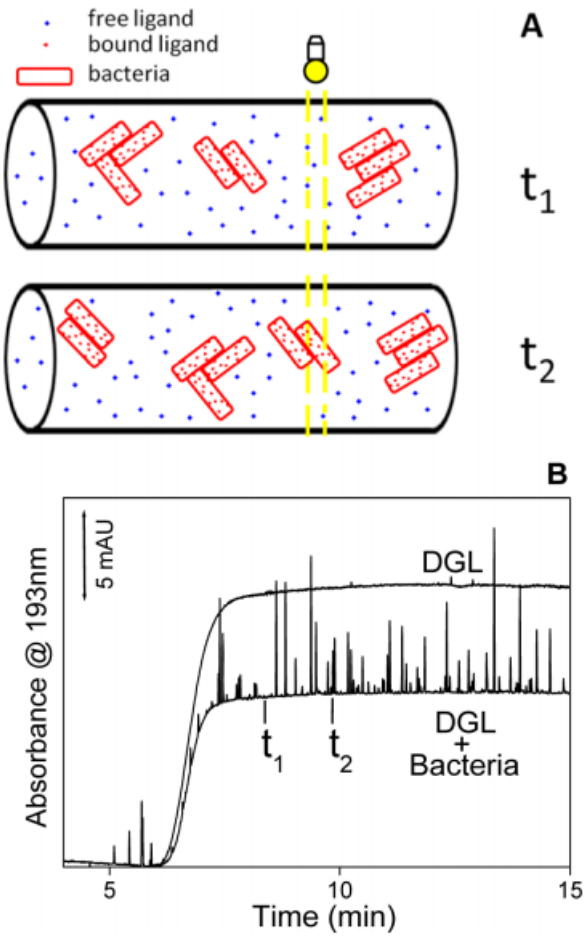

Figure 1.

Schematic representation during the FACCE of an equilibrated DGL-bacteria mixture at two different detection times (A). Electropherograms of a DGL (upper trace) or DGL-bacteria mixture (lower trace) obtained by FACCE (B). Experimental conditions: PDADMAC coated capillary 33.5 cm (8.5 cm to detector) × 50 µm i.d. Buffer electrolyte: 8 mM Tris + 6.5 mM acetic acid, 6.5 mM ionic strength, pH 7.4. Applied voltage: +2.5 kV with a cohydrodynamic pressure of +10 mbar. Samples are prepared in the BGE at final concentrations after mixture of 0.10 mg/mL for DGL G_2 and 1.59×10^8 cells/mL for *E. carotovora.*

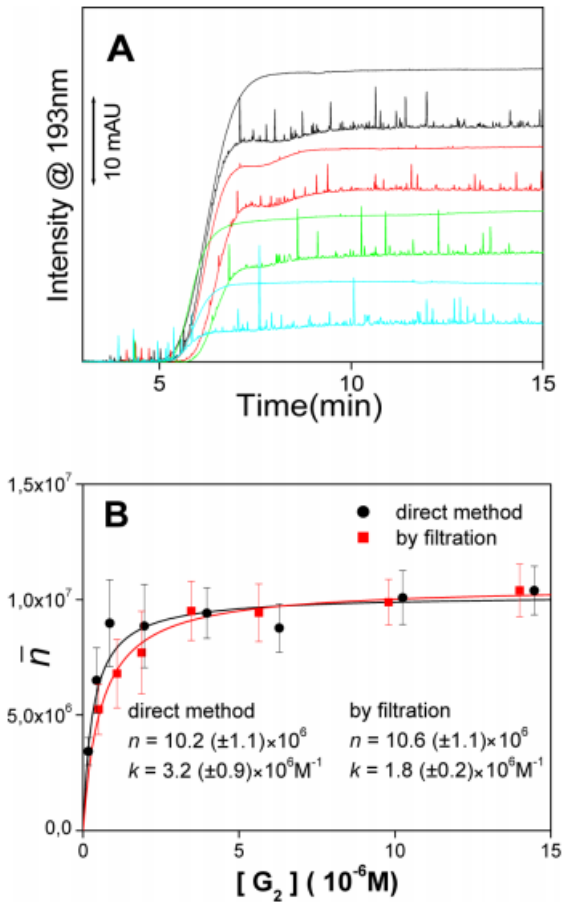

Figure 2.

FACCE electropherograms of G_2 (A, plain lines) or G_2-*E. carotovora* mixtures (A, hairy fronts) and the corresponding isotherm of adsorption (B, black circles). Experimental conditions: PDADMAC coated capillary 33.5 cm (8.5 cm to detector) × 50 µm i.d. Buffer electrolyte: 8 mM Tris + 6.5 mM acetic acid, 6.5 mM ionic strength, pH 7.4. Applied voltage: +2.5 kV with a cohydrodynamic pressure of +10 mbar (+20 mbar) from the injection end for the direct method (method with filtration, respectively). Samples are prepared in the buffer electrolyte at the following final concentrations: *E. carotovora* (1.59×10^8 cells/mL, i.e. 2.64×10^{-13} M) with G_2 at 200, 150, 100, 75, 50, 37.5, 25, and 12.5 mg/L for the direct method and E. carotovora (1.89×10^8 cells/mL, i.e. 3.14×10^{-13} M) with G_2 at 200, 150, 100, 75, 50, 37.5, and 25 mg/L for the method with filtration prior analysis. The red squares were obtained using sample filtration of the G_2-E. carotovora mixtures prior injection. All fronts are not presented in part A (75, 37.5, 25, and 12,5 mg/L in G2 not presented) for reasons of clarity. See section 6 in the SI for the error bars calculation

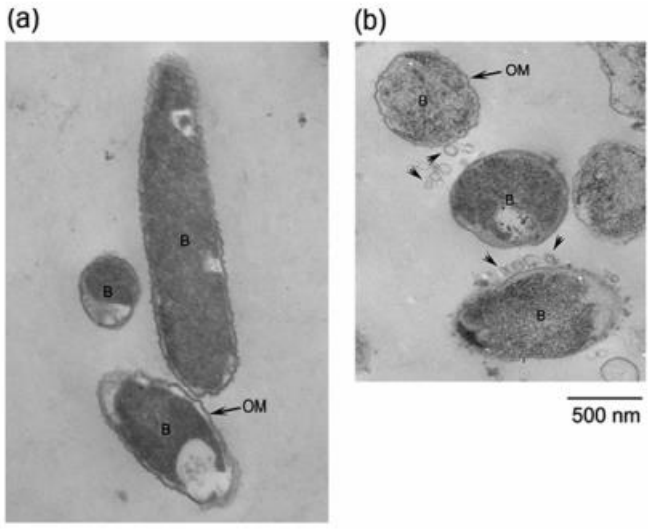

Figure 3.

Vesicles are released from the membranes of *E. carotovora* treated with DGL. Transmission electron microscopy of negatively stained *E. carotovora* cultures in stationary phase of growth. (a) After 3 h in Tris buffer, bacteria show an intact outer membrane (OM). Their size is in the range of 2 µm (length) × 0.5 µm (diameter). (b) After 3 h in Tris buffer and 10 min with DGL, many vesicles (arrow heads) are detaching from the outer membrane of the bacteria.

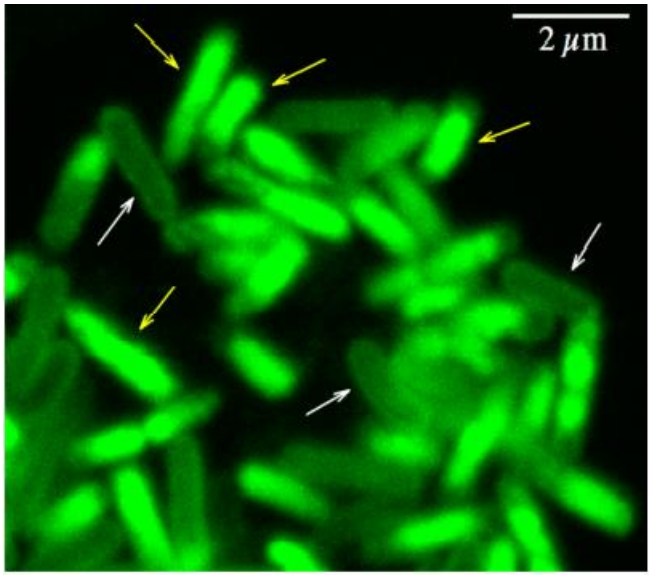

Figure 4.

Visualization of internalized G_2-FITC in *E. carotovora* after 1 h of contact between bacteria and G_2-FITC in Tris buffer. The picture was acquired by confocal microscopy; the image corresponds to one single focal plan. Fluorescence light corresponding to fluorescently labeled G_2 is observed at the cell membrane of all bacteria, and numerous bacteria show a massive intracellular accumulation of fluorescently labeled G_2. White arrows indicate some bacteria with G_2 mostly bound to the cell membrane; yellow arrows indicate some bacteria with high intracellular content of G_2.

	ligand	M_n (g/mol)[54]	n	n_{th}	n/n_{th}	n_{Lys}	k ($\times 10^6$ M^{-1})
Eriwinia carotovora	G_2[a]	8.6×10^3	$10.2 \pm 1.1 \times 10^6$	5.4×10^5	19 ± 2.0	$4.9 \pm 0.5 \times 10^8$	3.2 ± 0.9
	G_3[a]	22×10^3	$3.5 \pm 0.7 \times 10^6$	2.4×10^5	15 ± 2.5	$4.3 \pm 0.7 \times 10^8$	32 ± 4.7
	G_4[a]	65×10^3	$1.1 \pm 0.1 \times 10^6$	1.2×10^5	9 ± 0.8	$4.0 \pm 0.4 \times 10^8$	17 ± 6.2
	G_5[a]	172×10^3	$0.26 \pm 0.01 \times 10^6$	0.67×10^5	12 ± 0.2	$2.5 \pm 0.1 \times 10^8$	47 ± 7.0
	G_2[b]	8.6×10^3	$10.5 \pm 1.1 \times 10^6$	5.4×10^5	19 ± 2.0	$5.0 \pm 0.5 \times 10^8$	1 ± 0.1
polystyrene microbeads	G_2[a]	8.6×10^3	$8.9 \pm 0.7 \times 10^5$	20×10^4	5 ± 0.4	$4.3 \pm 0.3 \times 10^7$	0.25 ± 0.05
	G_3[a]	22×10^3	$3.2 \pm 0.2 \times 10^5$	8.8×10^4	4 ± 0.2	$4.0 \pm 0.2 \times 10^7$	3.5 ± 0.8
	G_4[a]	65×10^3	$1.4 \pm 0.1 \times 10^5$	4.3×10^4	3 ± 0.2	$5.1 \pm 0.4 \times 10^7$	15 ± 2.2
	G_5[a]	172×10^3	$0.45 \pm 0.03 \times 10^5$	2.3×10^4	2 ± 0.1	$4.3 \pm 0.3 \times 10^7$	9.4 ± 1.8

[a]6.5 mM ionic strength. [b]154 mM ionic strength. The relative errors were obtained by the software used for the least-square method.

Table 1.

Average Molar Mass Mn, Experimental Stoichiometry of the Interaction n, Theoretical Stoichiometry nth, Experimental Stoichiometry Expressed in Number of Lysine Residues nLys, and Binding Site Constant k for DGL with *E. carotovora* (or Polystyrene Microbeads)